# Observation of Laser Speckle Effects and Nonclassical Kinetics in an Elementary Chemical Reaction

Eric Monson and Raoul Kopelman

*Departments of Chemistry, Physics and Applied Physics, The University of Michigan, Ann Arbor, Michigan 48109-1055*

(Received 27 December 1999)

An experimental demonstration is provided for memory-based, nonclassical reaction kinetics in a homogeneous system with an elementary reaction, $A + B \rightarrow C$. A new reaction-kinetics regime is observed which is a direct consequence of speckles in the laser beam. However, in spite of the nonrandom, speckled initial distribution of reactant $B$, the long-time regime gives the first experimental demonstration of the asymptotic self-segregation ("Zeldovich") effect. Monte Carlo simulation results are consistent with the experiments.

PACS numbers: 82.40.–g, 05.40.–a

Pulse initiated reactions are of interest from astrophysics to laser chemistry and from radiation detectors to photodynamic cancer therapy. For the simplest case of an elementary, irreversible, diffusion-limited reaction, $A + B \rightarrow C$, the generally accepted scaling law is

$$(1/\rho - 1/\rho_0) \sim t^{\alpha}, \qquad \rho = \rho_A = \rho_B,$$

where $(1/\rho - 1/\rho_0)$ will be referred to as the *reaction progress,* and $\rho_0$ is the density at $t = 0$. Classical textbooks, from chemistry to solid-state physics [1], give $\alpha = 1$. Nonclassical kinetics [2] gives the asymptotic ($t \rightarrow \infty$) relations

$$\alpha = d/4 \qquad d \leq 4,$$
$$\alpha = 1 \qquad d \geq 4$$

for initially random distributions (the most widely studied case), irrespective of initial $\rho$ [3,4]. We note that the nonclassical effects we deal with result from the preservation of a "memory" of the initial spatial reactant distribution, which is not limited to any certain concentration range. (Classical behavior requires thorough, continuous stirring, i.e., rerandomization.) So far there has been no experimental verification of these nonclassical results. Furthermore, we believe that all experimental verifications of the classical result ($\alpha = 1$) involved stirred (i.e., constantly rerandomized) systems [5]. However, most real-life applications, from surface catalysis to geochemistry to biochemistry, do not allow stirring. Nevertheless, much of the solid-state and surface science literature still uses the classical formalism; e.g., exciton annihilation is assumed to be proportional to the square of the exciton density, or the rate of electron-hole recombination is assumed to be linear in both electron and hole densities [1]. We thus felt the need for some controlled experiments (where there is no convection or stirring) aimed at observing nonclassical behavior in an elementary $A + B$ reaction.

While much theoretical work has been done on the initially random and geminate [6] reaction systems, only recently has consideration been given to other initially correlated systems. The theoretical work by Lindenberg and co-workers [7,8] showed the dramatic effects of varying $t = 0$ spatial correlations in the $A + B \rightarrow 0$ system, resulting in a hierarchy of *reaction progress* time regimes, each with a different scaling law. For example, in the case of a fractal initial distribution [8], where the particles are landed on a one-dimensional lattice in a fractal pattern, a very slow reaction rate is observed due to the overabundance of long wavelength components in the spatial fluctuations of the reactant distribution (compared to the flat distribution of a random system).

To our knowledge, there are no previous experimental studies on nongeminate initially correlated systems. In the work described in this Letter a hierarchy of kinetic behaviors has indeed been observed for a simple, elementary, binary reaction. The $t = 0$ spatial correlation utilized in the present work is similar in spirit, though very different in detail, from those described above [7,8]. Here reactant $A$ is randomly distributed (standard chemical solution), while the initial distribution of reactant $B$ (photochemically released from a "cage" molecule) is determined by laser speckles [see Fig. 1(a)]. The reaction $A + B \rightarrow C$ is studied by time resolved fluorescence (from the product $C$). Specifically, $A$ is a low fluorescence dye ("Calcium Green-1"™), $B$ is $Ca^{2+}$, and $C$ is the highly fluorescent $AB$ adduct.

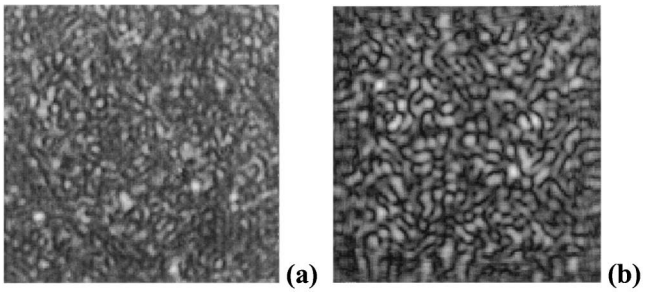


FIG. 1. (a) Experimental CCD image ($65 \times 65$ $\mu$m region) showing the UV intensity distribution on a section of the delivery fiber face (pattern highly reproducible from flash to flash). (b) Matlab generated speckle intensity pattern (size is shown for comparison with the experimental image).

 0031-9007/00/85(3)/666(4)$15.00 

Each experimental run is initiated with a speckled pulse of UV light generated by frequency tripling a ~10 ns pulse from a Nd:YAG laser to 354 nm. This beam then passes through a UV filter (Schott UG-1) followed by neutral density filters for fine power control. Fused silica fiber with a 500 $\mu$m core diameter is used for delivery of the light to the sample atop an Olympus IX-70 inverted fluorescence microscope [9]. A 100 W mercury arc lamp and filters are used for fluorescence excitation in an epi-illumination geometry, and the signal is delivered to a Hamamatsu photomultiplier tube with variable high voltage supply. After current to voltage conversion the signal is recorded by a digital oscilloscope—data acquisition being triggered by a $Q$-switch output pulse from the laser.

Samples are held in 10 to 100 $\mu$m inside diameter fused silica capillaries (Polymicro Technologies). Details of the illumination geometry are shown in Fig. 2 [10]. The sample region pulsed is about twice as wide as the segment monitored for the kinetics so as to avoid effects of diffusion in and out of the UV pulsed section. We would not expect surface charges to have a large effect on our results, because at 10 m$M$ ionic strength (characteristic of our aqueous environment) the surface charges will be shielded to about 2% by $\cong$10 nm from the wall [11], which is 0.02% of the capillary diameter in most cases. A single laser pulse triggers data acquisition and initiates the reaction. To include the equal $A$ and $B$ population point, the UV pulse energies were varied within each series of experiments using the neutral density filters.

DM-Nitrophen (DMN) [12] was chosen as the cage molecule because it combines very strong binding (relative to the calcium dyes) with a good product of extinction coefficient and quantum efficiency for uncaging. Calcium Green-1™ (CG1), from Molecular Probes, was chosen as the reporter reactant for most experiments. Its calcium adduct has reasonably strong calcium binding, visible light excitation (so that the fluorescence monitoring does not uncage calcium), and a good ratio of bound to unbound fluorescence intensity [13].

The choice of chemical environment was tailored to kinetics work rather than the more standard physiological conditions used with these compounds for biochemical sensing. The parent compounds (BAPTA [14] for CG1 and EDTA for DMN) exhibit environmentally sensitive binding [15]. DMN has a strong increase in calcium binding strength through the basic $p$H range, while lowered ionic strength increases CG1 binding more significantly than DMN. A Tris-HCl (8.3 m$M$) -KCl (2 m$M$) buffer, with $p$H 8.5 and ionic strength of 11 m$M$, was prepared and titrations were conducted to both confirm the general effects of changing ionic strength and $p$H and to set the initial calcium levels (neither chemical is supplied bound to calcium). Some sort of "reversible photobleaching" of the dye was observed with each UV pulse [16]. It was found that $p$-phenylene diamine [17] was the only compound, out of many tested, which eliminated the effect.

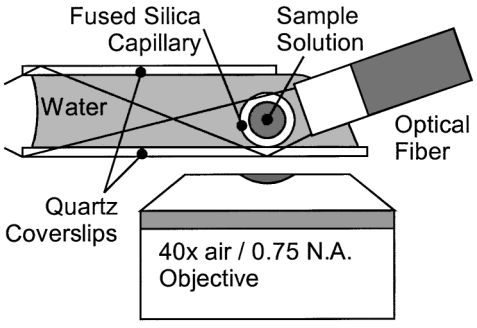


FIG. 2. Capillary sample chamber (side-on) with optical fiber UV pulse delivery. Total internal reflection and close index matching reduce stray light into the microscope objective and subsequent detection system.

Linearly spaced voltage (intensity) data were smoothed with the same routine as used in Ref. [18]. The algebraic increase in bin size with time results in evenly spaced data points in time on a log-log plot without "throwing out" any data. The fluorescence of the bound and unbound forms of the dye differ by a constant multiplicative factor, which depends on the specific experimental conditions, so the standard sensor dye relationship was used: $[F_{\max} - F(t)] = \text{const} \times A(t)$, where $F_{\max}$ is the fluorescence intensity that would be achieved if all the dye were bound with calcium within a given region, and $A(t)$ is the time dependent reactant density. Photobleaching and local concentration fluctuations make $F_{\max}$ difficult to measure with great certainty, so this becomes the largest contributor to errors in the calculation of the *reaction progress,* $(1/\rho_A - 1/\rho_{A0})$.

Figure 3 shows two typical series of *reaction progress* vs time measurements with various UV uncaging pulse powers, in two different viscosity environments. Experiments conducted in a standard, aqueous buffer solution, compared to a solution with 50% wt:wt glycerol, are shown to exhibit identical behaviors but with the rate features shifted in time by a factor of 6, which is close to the viscosity ratio. This verifies the contribution of the diffusion limitation to the product formation rate features. In both sets of curves, the last few data points show the slowing of fluorescent product formation as the binding of calcium ions shifts from the dye back to unphotolyzed cage molecules, and early time behavior in the reactions is masked somewhat by a spike in the signal due to detected residual uncaging light (which falls to background levels by 20–70 $\mu$s, depending on pulse power). The fluorescence shows a variable time structure: an early, fast rate of product formation, followed by a slowing of the rate, then by another rise in rate. The values of these slopes vary with reactant stoichiometry, but if we focus on the center data set, we see that the mid-time, slower region has a slope around $\frac{1}{8}$ (much slower than any previously established rate), and the later-time, fast region has a slope of about $\frac{3}{4}$ (which matches the predicted asymptotic behavior of the "Zeldovich," *three-dimensional,* $A + B \rightarrow C$ case).

Neither in the classical case nor in the usual random $A + B$ diffusion limited nonclassical case are so many different behavior regimes expected. Both of these theories predict a faster, monotonic product increase, lacking this mid-time, extremely slow rate region. No adjustment of initial densities or additional model complexity, as in reversibility and competition between cage and dye (through simulations), could account for the fast-slow-fast rate behavior seen in the experimental results. Control experiments have been conducted with a nonspeckled uncaging pulse source: a xenon flash lamp. Replacing the laser pulse with that of a flash lamp (no speckles) removed the mid-time anomalous rate regime.

We tested a very simple model of speckled illumination in computer simulations to see if such a speckled initial distribution is *sufficient* to explain the experimental anomalies. Indeed, the introduction of these types of correlations in the initial spatial distribution led to very similar results between the simulations and experiments. The $A + B \rightarrow C$ reaction was tested with an initially random $A$ spatial distribution and a speckled $B$ distribution. Monte Carlo methods were used to simulate the $A + B \rightarrow C$ anomalous reaction kinetics in *one* and *two dimensions,* modeling the reaction and diffusion in the usual way [19]. In brief, particles were landed on the lattice with no excluded volume conditions, the $A$'s randomly, and the $B$'s randomly within speckled probability maps which had a value on each lattice site, simulating a local UV pulse intensity in the experimental setup. All members of each particle type were moved once within each time step (using cyclic boundary conditions), followed by a check for occupation of the new sites by particles of the other type and product formation ($C$). One of our approaches to simulated speckle generation is similar to that of Fujii *et al.* [20], using a slightly smoothed, Gaussian random rough surface to vary the phase of a coherent plane wave, after which the resultant speckled intensity pattern is calculated some distance from the surface. Figure 1(b) shows one such simulated speckle pattern.

Figure 4 shows some speckled simulation results. The similarity to the experimental results in Fig. 3 is obvious, as well as the contrast with the standard, initially random case (labeled solid lines). Both *one-* (inset) and *two-dimensional* results are presented with two speckle sizes and equal initial $A$ and $B$ populations, while the 2D case includes illustrations of $B$:$A$ initial density ratios of 1.5:1, 1:1, and 1:1.5 (simulating the use of varying UV uncaging powers in the experiments).

In the simulated speckled case, we also observe that during the second rise in reaction rate both the 1D and 2D curves approach the $t^{d/4}$ power law slope characteristic of the initially random $A + B \rightarrow 0$ (Zeldovich) case [3,4]. In the initially random case, the crossover to this dimension-dependent behavior happens at a characteristic ratio of the density to the initial density [21]. In this speckled case, however, the crossover time ($t_c$) seems to be dependent on the speckle size, proceeding as the Einstein diffusion law scaling of $t_c \sim \langle x^2 \rangle$. In the two-dimensional case we see the crossover to the dimension-dependent regime at a density of about $\rho_A/\rho_{A0} \approx (0.15/0.4) = 0.375$, much earlier than the ratio of 0.03 reported for the initially random case

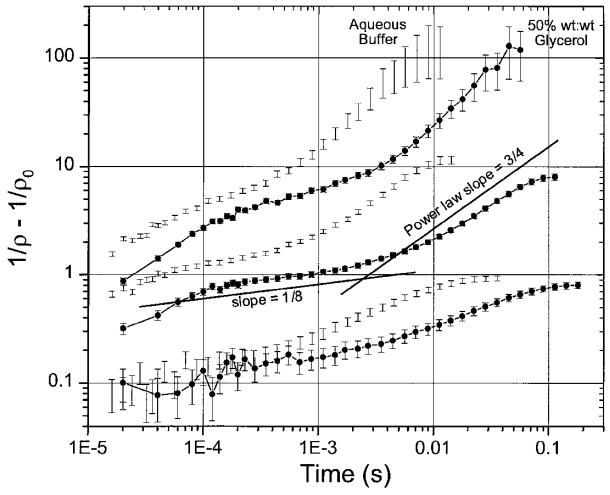


FIG. 3. Experimental *reaction progress* of calcium-dye reaction in 50% wt:wt buffer-glycerol solution (solid circles) and in buffer without glycerol (bars). UV pulse energy varies by about a factor of 3 (ND 0.5) between curves in each set (low to high energy from bottom to top). The solid lines are presented as a guide to the eye, the first having a power law slope of $\frac{1}{8}$, and the second having a power law slope of $\frac{3}{4}$ (equal to the *three-dimensional* Zeldovich asymptotic rate for the $A + B \rightarrow C$, equal density, annihilation reaction).

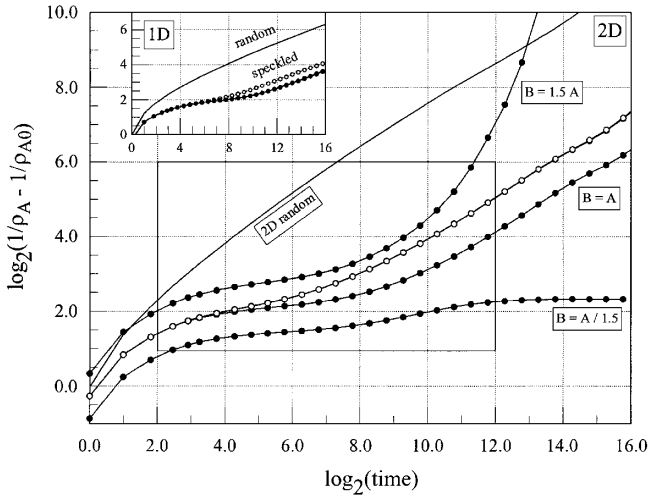


FIG. 4. *One-* (inset) and *two-dimensional* simulation results (10 run averages) for the *reaction progress* using Matlab generated speckled initial $B$ conditions. Open symbols are for average size 64 speckles, and filled symbols correspond to average size 128 speckles. Initially random cases (solid lines) are shown for contrasting behavior, and for reference to the $t^{0.5}$ and $t^{0.25}$ power law slopes. $B/A$ ratios of 1.5:1, 1:1, and 1:1.5 are included in 2D (simulating UV pulse energy variation) and the box is a guide (in time and in *reaction progress* range) for comparison with the experimental results in Fig. 3.

[21]. The presegregation which is built into the speckled initial conditions seems to bring on the fully segregated Zeldovich behavior much earlier.

Further specific insight is provided by spatial analyses conducted on the speckled initial condition simulations. The initial, fast regime is seen to stem from spatial fluctuations inherent in the random distribution of reactants, combined with the locally high and low extremes in $B$ concentration formed by the speckled intensity. This leads to a quasiclassical rate which persists until the characteristic length scale of the particle distribution reaches that of the speckles themselves. During the mid-time, extremely slow rate regime, it is the progress through spatial scales characteristic of the speckles which governs the *reaction progress* temporal scaling. The speckles create an overabundance of long-wavelength components in the spatial fluctuations of the reactant distribution (compared to a flat, random distribution), causing a *reaction progress* slowdown similar to the case of a fractal distribution [8], but of finite duration. Once the size scale of the reactant segregation proceeds beyond the limits inherent in the speckles, the rate again increases. Since the speckles do not have any long wavelength contribution beyond these scales, this last regime has the characteristic Zeldovich behavior of an initially random distribution reaction, where at late times the reactants are segregated and these segregated spatial regions keep growing through a flat fluctuation spectrum landscape.

Summarizing, we have successfully demonstrated a model experimental system for the nonstirred elementary $A + B \rightarrow C$ reaction, along with the effects of a laser speckled initial reactant distribution. In fact, what seemed to be an anomalous rate behavior when compared to the well studied initially random case is a result of the strong dependence of the reaction behavior on its memory of the correlated initial reactant distribution. Thus, a simple speckle model accounts well for the observed anomaly. Our results also seem to exhibit, for the first time, an experimental realization of the nonclassical Zeldovich asymptotic rate behavior. These experiments highlight the necessity of taking modern nonequilibrium reaction kinetics theory seriously, as even in this case of a somewhat reversible reaction, the effects of initial reactant distribution and lack of mixing are dramatic.

We gratefully acknowledge funding from NSF Grant No. DMR-9900434. Thanks also go to Dr. Anna Lin (reaction kinetics and Matlab), Dr. Susan Barker and Dr. Heather Clark (sensor molecules), and Dr. Andrea Stout (dye behavior artifacts).

[1] For example, P. Atkins, *Physical Chemistry* (W. H. Freeman & Co., New York, 1998); C. Kittel, *Introduction to Solid State Physics* (John Wiley & Sons, Inc., New York, 1967).

[2] R. Kopelman, Science **241**, 1620 (1988); *Proceedings of Models of Non-Classical Reaction Rates, Bethesda, MD, 1991,* edited by J. L. Lebowitz [J. Stat. Phys. **65**, Nos. 5/6 (1991)]. This conference was in honor of George Weiss.

[3] A. A. Ovchinnikov and Y. B. Zeldovich, Chem. Phys. **28**, 215 (1978).

[4] D. Toussaint and F. Wilczek, J. Chem. Phys. **78**, 2642 (1983).

[5] See, e.g., P. Argyrakis and R. Kopelman, J. Phys. Chem. **93**, 225 (1989).

[6] For geminate initial distributions, where $A$ and $B$ are landed (at $t = 0$) as nearest neighbor pairs, $\alpha = d/2$ for $d \leq 2$ and $\alpha = 1$ for $d \geq 2$ [4].

[7] K. Lindenberg, P. Argyrakis, and R. Kopelman, in *Noise and Order: The New Synthesis,* edited by M. Millonas (Springer, New York, 1996), Chap. 12, p. 171.

[8] K. Lindenberg, A. H. Romero, and J. M. Sancho, Int. J. Bifurcation Chaos **8**, 853 (1998).

[9] Fiber temporal stretching of the UV pulses has been neglected since the pulses are quite long (10 ns) and the absorption cross section of the cage changes only slightly with the time scale of excitation. See J. W. Walker *et al.,* J. Am. Chem. Soc. **110**, 7170 (1988).

[10] The experimental setup limits distortions of the speckle pattern by the capillary since the $n = 1.48$ capillary is surrounded by and contains $n = 1.33$ water. But, we make no specific claims about the details of the speckle pattern (e.g., size of speckles or lack of distortion to the pattern).

[11] R. J. Hunter, in *Zeta Potential in Colloid Science* (Academic Press, New York, 1988).

[12] J. H. Kaplan and G. C. R. Ellis-Davies, Proc. Natl. Acad. Sci. U.S.A. **85**, 6571 (1988).

[13] M. Eberhard and P. Erne, Biochem. Biophys. Res. Commun. **180**, 209 (1991).

[14] R. Y. Tsien, Biochemistry **19**, 2396 (1980). BAPTA denotes 1,2-bis($o$-aminophenoxy)ethane-$N, N, N', N'$-tetra-acetic acid.

[15] S. M. Harrison and D. M. Bers, Biochim. Biophys. Acta **925**, 133 (1987). EDTA denotes ethylenediamine tetra-acetic acid; Tris denotes Tris(hydroxymethyl)-aminomethane.

[16] A. L. Stout and D. Axelrod, Photochem. Photobiol **62**, 239 (1995).

[17] G. D. Johnson *et al.,* J. Immunol. Meth. **55**, 231 (1982); K. Valnes and P. Brandtzaeg, J. Histochem. Cytochem. **33**, 755 (1985).

[18] A. L. Lin, E. Monson, and R. Kopelman, Phys. Rev. E **56**, 1561 (1997).

[19] P. Argyrakis, Comput. Phys. **6**, 525 (1992).

[20] H. Fujii, J. Uozumi, and T. Asakura, J. Opt. Soc. Am. **66**, 1222 (1976).

[21] P. Argyrakis, R. Kopelman, and K. Lindenberg, Chem. Phys. **177**, 693 (1993).